Caspase-dependent initiation of apoptosis and necrosis by the Fas receptor in lymphoid cells: onset of necrosis is associated with delayed ceramide increase

Claudio A. Hetz[1], Martin Hunn[2], Patricio Rojas[1], Vicente Torres[1], Lisette Leyton[1] and Andrew F. G. Quest[1,*]

[1]Instituto de Ciencias Biomédicas, Facultad de Medicina, Universidad de Chile, Santiago, Chile
[2]Institute of Biochemistry, University of Lausanne, Switzerland
*Author for correspondence (e-mail: aquest@machi.med.uchile.cl)

Accepted 4 September 2002
Journal of Cell Science 115, 4671-4683 © 2002 The Company of Biologists Ltd
doi:10.1242/jcs.00153

Summary

Engagement of the Fas receptor promotes apoptosis by activation of caspases. In addition, alterations in plasma membrane lipid orientation and intracellular ceramide levels are often observed. In A20 B-lymphoma cells, FasL-induced cell death and phosphatidylserine (PS) externalization were completely prevented by the generic caspase inhibitor z-VAD-fmk. By contrast, the caspase-3 inhibitor Ac-DEVD-cho only partially restored cell viability and had no effect on surface exposure of PS. Flow cytometric analysis after FasL treatment identified two populations of dead cells. In one, death was dependent on caspase-3 and paralleled by DNA fragmentation and cell shrinkage. In the second, death occurred in the absence of caspase-3 activity and apoptotic features but was also blocked by zVAD-fmk. By morphological criteria these were identified as apoptotic and necrotic cells, respectively. Using fluorescent substrates, caspase-3 activity was detected only in the apoptotic cell population, whereas caspase-8 activity was detected in both. Both forms of caspase-8-dependent cell death were also detected downstream of Fas in Jurkat T-cells, where Fas-dependent PS externalization and delayed ceramide production, which is similar to results shown here in A20 cells, have been reported. However, for Raji B-cells, lacking lipid scrambling and ceramide production in response to Fas activation, only apoptosis was detected. Short-chain C2- or C6-ceramides, but not the respective inactive dihydro compounds or treatment with bacterial sphingomyelinase, induced predominantly necrotic rather than apoptotic cell death in A20 B-, Raji B- and Jurkat T-cells. Thus, delayed elevation of ceramide is proposed to promote necrosis in those Fas-stimulated cells where caspase-8 activation was insufficient to trigger caspase-3-dependent apoptosis.

Key words: Lymphoid cells, Fas, Apoptosis, Necrosis, Caspases, Ceramide

Introduction

The interaction between FasL and the Fas (Apo-1/CD95) receptor plays an essential role in the control of T- and B-cell activity and maintenance of immunological tolerance. Repeated antibody stimulation of $CD4^+$ T-cells results in high levels of Fas and FasL expression and, as a consequence, these cells die (Abbas, 1996; Cornall et al., 1995; Matiba et al., 1997; Nagata, 1997). Likewise, Fas is involved in the elimination of active or autoreactive B-lymphocytes (Cornall et al., 1995; Nagata, 1997).

FasL binding stabilizes the trimeric form of the Fas receptor, thereby allowing recruitment of the Fas-associated death domain (DD)-containing protein (FADD). FADD then binds to and activates caspase-8, an initiator caspase, which in turn activates downstream effector caspases, including caspase-3 (Martins and Earnshaw, 1997; Nagata and Golstein, 1995; Suda et al., 1993). As a consequence, many cellular proteins are degraded, leading to cell death.

Depending on the cell type and the stimulus, a cell may die either by apoptosis or necrosis. Apoptosis is characterized by chromatin condensation, internucleosomal degradation of the DNA, cell shrinkage and disassembly into membrane-enclosed vesicles as a consequence of caspase activation (Rathmell and Thompson, 1999). Apoptotic and necrotic cells are both recognized by phagocytes, but only apoptotic cells are eliminated without release of cytosolic components to the environment, thereby preventing an inflammatory response (Fadok et al., 2000; Sauter et al., 2000). Necrosis, on the other hand, is characterized by swelling of the cells and organelles, resulting ultimately in disruption of the cell membrane and cell lysis (Majno and Joris, 1995).

Initially, FasL was only thought to trigger cell death by apoptosis. Recently, however, inhibition of Fas-induced apoptosis in L929 fibrosarcoma cells by a caspase inhibitor lead to necrosis mediated by oxygen radicals (Vercammen et al., 1998a; Vercammen et al., 1998b). Also, primary activated T cells can be efficiently killed by FasL, TNF-α and TRAIL in the absence of active caspases (Holler et al., 2000). These results suggested that Fas, like TNFR-1 (Laster et al., 1988), triggers apoptotic or necrotic death.

Treatment with FasL, TNF-α or IL-1β leads to formation of ceramide, in addition to caspase-3 activation (Garcia-Ruiz et

al., 1997; Gudz et al., 1997). Ceramide reportedly modulates the activity of a large number of proteins (Heinrich et al., 1999; Venkataraman and Futerman, 2000) and, in doing so, may promote apoptosis. In addition, ceramide directly modulates mitochondria function, for instance by inhibiting the mitochondrial respiratory complex III (Garcia-Ruiz et al., 1997; Gudz et al., 1997; Quillet-Mary et al., 1997). Sphingomyelin hydrolysis by either neutral (nSMase) or acidic sphingomyelinases (aSMase) is generally implicated in ceramide production (Hannun et al., 1996; Kolesnick and Kronke, 1998).

Treatment of lymphoid cells with FasL induces elevation of intracellular ceramide levels. However, data are conflicting with regard to the kinetics of the ceramide response and the SMases involved downstream of Fas. Some authors have found a rapid transient response within minutes to an hour that depends on initiator caspases, like caspase-8, and has been attributed to activation of an aSMase (Cifone et al., 1995; Genestier et al., 1998). Alternatively, others have reported that apoptosis of lymphoid cells is generally accompanied by caspase-8-dependent, delayed ceramide production (after several hours) owing to the hydrolysis of plasma membrane sphingomyelin as a consequence of phospholipid scrambling. Increases in ceramide levels followed the kinetics of nuclear fragmentation and occurred after cytochrome c release or caspase-3 activation. In addition, Raji B-cells, which do not produce ceramides upon Fas activation, display apoptotic features in mitochondria and the nucleus (Tepper et al., 1997; Tepper et al., 2000). These observations argue strongly against a role for ceramides in triggering apoptosis. Also, data obtained using aSMase knock-out mice and overexpression of a nSMase have failed to implicate these SMases in either Fas-induced ceramide production or apoptosis of B- and T-cells (Brenner et al., 1997; Cock et al., 1998; Tepper et al., 2001). Thus, although evidence abounds suggesting that ceramide can promote apoptosis, the extent to which ceramide formation is essential remains controversial and appears to depend largely on the cellular system used (Cifone et al., 1995; Hannun et al., 1996; Hofmann and Dixit, 1998).

Here we investigated some of these questions, with a focus on A20 B- and Jurkat T-lymphoma cells, where cell death is readily induced with recombinant, soluble FasL. We observed that FasL stimulated two distinct types of caspase-8-dependent cell death: apoptosis that occurred via activation of caspase-3 and necrosis which, like phosphatidylserine (PS)-externalization, was caspase-3 independent. On the other hand, FasL also significantly increased ceramide levels after 3 hours in A20, as previously described for Jurkat T-cells. Treatment with cell-permeable ceramides or bacterial SMase led to necrosis in both cell types. In Raji B-cells, lacking ceramide production owing to absence of lipid scrambling (Tepper et al., 2000), Fas activation triggered only apoptosis at all antibody concentrations tested, whereas cell-permeable ceramides and bacterial SMase promoted necrosis. In the presence of FasL, addition of cell-permeable ceramides only promoted necrosis in A20 and Jurkat cells when added within the first 4 hours after FasL. Thus, Fas-induced lipid scrambling and delayed elevation of intracellular ceramide levels are suggested to promote necrosis in cells where FasL failed to trigger caspase-3-dependent apoptosis.

Materials and Methods

Materials

The detergents nonidet P-40 (NP-40), sodium deoxycholate and 3-[(3-Cholamidopropyl)-dimethylammonio]-1-propanesulfonate (CHAPS) and bacterial SMase (Staphylococcus aureus) were from Sigma (Buchs, Switzerland). The fluorogenic caspase substrates (Ac-DEVD-amc, Ac-YVAD-amc) and caspase inhibitors (Ac-DEVD-cho, Ac-YVAD-cho, zVAD-fmk) were from Alexis Biochemicals (Läufelfingen, Switzerland). The cell-permeable caspase-3 substrate FAM-DEVD-fmk was from Promega (Madison, WI) and the cell-permeable caspase-8 substrate FAM-LETD-fmk from Intergen (New York, NY). C6-ceramide, dihydro-C6-ceramide, C2-ceramide and dihydro-C2-ceramide were from Biomol Research Laboratories Inc. (Wangen, Switzerland). Brain ceramides and dioctanoylglycerol were from Avanti Polar Lipids Inc. (Alabaster, AL). n-Octyl-β-D-glycopyranoside ULTROL grade was from Calbiochem (Lucerne, Switzerland). Protease inhibitors, RNAse A and annexin-V binding kit were from Boehringer Mannheim/Roche Biochemicals (Basel, Switzerland). Cell medium, fetal calf serum and antibiotics were from GIBCO-BRL (Basel, Switzerland). Organic solvents of the highest quality available were from Fluka (Buchs, Switzerland). Soluble recombinant human FasL was from Apotech SA (Geneva, Switzerland). Anti-human Fas antibodies (clone IPO-4) were from Kamaya Biochemical Company (Seattle, WA).

Cell culture

A20, A20R and M12 cells (kindly provided by Jürg Tschopp, Institute of Biochemistry, University of Lausanne, Switzerland) were cultured in DMEM supplemented with 10% fetal calf serum, antibiotics (10,000 U/ml Penicillin, 10 μg/ml streptomycin) and 50 μM ethanol-2-thiol at 37°C and 5% CO_2. Ramos, Daudi and Raji human B-lymphoma lines and the EBV-transformed human B-lymphoblast cells GES and LM, all provided by Maria-Rosa Bono (Faculty of Basic Sciences, University of Chile), were cultured in RPMI supplemented with 10% fetal calf serum and antibiotics at 37°C, 5% CO_2.

In vitro caspase-3/caspase-1 assay

A20 and Jurkat cells (0.5×10^6 cells) were treated with FasL for 0-8 hours at 37°C. To test the effect of C6-ceramide or caspase inhibitors, cells were preincubated for 30 minutes. Then caspase activity was measured using a previously described protocol (Hetz et al., 2002) modified from Boldin et al. (Boldin et al., 1996).

In situ caspase-3/caspase-8 assay

Caspase activity was detected using the caspase-3 substrate FAM-DEVD-fmk (Promega, Madison, WI) or the caspase-8 substrate FAM-LETD-fmk (Intergen, New York, NY), following instructions from the manufacturer, by flow cytometry (FACS; Becton Dickinson, Mountain View, CA) and the Cell Quest program.

Viability assays

Cell viability was analyzed by FACS as described before (Hetz et al., 2002). A20 cells were incubated with either C6-ceramide or dihydro-C6-ceramide (DH-C6-ceramide) at the concentrations indicated for up to 16 hours at 37°C. For inhibition experiments, cells were preincubated for 30 minutes without or with the caspase inhibitors Ac-DEVD-cho (100 μM), Ac-YVAD-cho (100 μM) or zVAD-fmk (10 μM). Then FasL was added, and cells were incubated for another 16 hours at 37°C. Cells were harvested and stained with 10 μg/ml of propidium iodide (PI) for determination of cell viability. For DNA content analysis cells were permeabilized with methanol and stained with PI. Samples containing roughly 1×10^4 cells were analyzed by FACS using the Cell Quest program. Alternatively, cells were sorted

by FACS using PI fluorescence emission as the parameter for selection and nuclear morphology was analyzed by confocal microscopy as described below.

Cell viability was also quantified by alternative methods using the reagents 3-(4,5-dimethylthazol-2-yl)-5-3-carboxymethoxy-phenyl)-2-(4-sulfophenyl)-2H-tetrazolium (MTS) and phenazine methosulfate (PMS) according to the recommendations of the supplier (Promega, CellTiter96® Aqueous).

Diacylglycerol kinase assay

Ceramide concentrations were determined in 5×10^6 cells as previously described (Preiss et al., 1987; Walsh and Bell, 1986) using brain ceramide (Avanti Polar Lipids, Alabaster, AL) as a standard. Determinations were done in triplicate in each experiment. On average (n=6), basal ceramide and diacylglycerol levels in A20 or A20R cells were 2.9±1.0 pmol/nmol lipid phosphate (or 132±55 pmol per 5×10^6 cells) and 14±3.2 pmol/nmol lipid phosphate (or 630±184 pmol per 5×10^6 cells), respectively. These values are referred to as 100%.

DNA fragmentation assay

A20 cells (1×10^6/ml) were incubated in complete medium with FasL, C6-ceramide, dihydro-C6-ceramide or combinations thereof for 4 hours at 37°C. For the inhibition experiments, cells were preincubated for 30 minutes with caspase inhibitors. Subsequently, cells were harvested by brief centrifugation and lysed by addition of 100 μl phenol/chloroform/isoamylalcohol (25:24:1) and centrifuged. Then, 17.5 μl of the aqueous phase were mixed with 2 μl 10× buffer H (50 mM Tris-HCl pH 7.5, 10 mM $MgCl_2$, 100 mM NaCl, 1 mM dithioerythrol) and 0.5 μl RNase A solution (500 mg/ml), incubated for 30 minutes at 37°C and analyzed by electrophoresis on a 2% agarose gel containing 0.5 mg/ml ethidium bromide. DNA bands were visualized by exposure to UV light.

Assessment of chromatin condensation and morphological changes

Cells were treated as described previously (viability assays) and stained after 16 hours cells with PI (1 μg/ml) for 5 minutes. After washing twice in PBS, cells were treated with glycerol-DABCO and viewed by an SLM-400 Carl Zeiss confocal microscopy upon excitation at 543 nm using a 570 nm emission filter (UACI, ICBM, University of Chile). As a control, cells were permeabilized by addition of 500 μl ice-cold ethanol and incubated for 10 minutes at –20°C before staining with PI. A total of 200 cells were analyzed. Alternatively, cells were washed in PBS and fixed with 3% glutaraldehyde, 100 mM Na-cacodylate for 1.5 hours at 4°C. After post-fixation in 1% AsO_4 and dehydration, cells were embedded in EPSON 812 resin. Sections were stained with uranyl acetate and lead citrate and were observed in a Zeiss TEM 109 Electron Microscope (Electron Microscopy Center, ICBM, Department of Morphology, University of Chile).

Quantification of phosphatidylserine exposure

Presence of phosphatidylserine in the outer leaflet of the plasma membrane was detected following instructions of the manufacturer by flow cytometry using FITC-coupled annexin V (annexin V-FITC) and 5×10^3 cells per experiment.

Results

FasL-induced caspase-3 activation and apoptosis in A20 cells.

To study the signaling events in FasL-induced apoptosis, the murine B-lymphoma cell line A20 was initially employed as a model system, together with FasL-insensitive A20R cells as controls. Resistance to FasL-induced cytotoxicity in the latter case is probably due to downregulation of Fas (Hahne et al., 1996). Incubation of A20 cells with recombinant soluble human FasL for 16 hours induced cell death in a concentration-dependent fashion (not shown), whereby 90% dead cells were observed with 100 ng/ml (Fig. 1A). No decrease in cell viability was observed in A20R cells under similar conditions (data not shown).

Addition of 100 μM of the caspase-3 inhibitor Ac-DEVD-cho following FasL treatment increased cell viability by 30%, whereas incubation with 100 μM of the caspase-1 inhibitor Ac-YVAD-cho did not protect A20 cells. Pre-incubation of cells with the broad-range caspase inhibitor zVAD-fmk (10 μM) completely protected cells against FasL-induced cell death (Fig. 1A, see below Fig. 5). These observations are consistent with the interpretation that activation of caspase-8, an initiator caspase upstream of caspase-3, represents an early event triggered by Fas, leading to cell death. Interestingly, inhibition of caspase-3 and related caspases only partially restored cell viability upon treatment with FasL.

Caspase-3 activation, measured directly by monitoring cleavage of the fluorogenic substrate Ac-DEVD-amc, was detectable within 2 hours and rose until 8 hours after addition of FasL to over 10-fold, eight-fold or two-fold baseline values in the presence 100, 32 or 10 ng/ml FasL, respectively (Fig. 1B). During the same period, no activation of caspase-1 was detectable using the fluorogenic substrate Ac-YVAD-amc (data not shown). Western blot analysis, using a caspase-3-specific antibody revealed that pro-caspase-3 protein levels began to decline within 1 hour of treatment with FasL (100 ng/ml) and essentially disappeared within 2-3 hours, as did polyADP-ribose polymerase, a caspase-3 target (data not shown).

A hallmark of apoptosis is the generation of DNA fragments of defined length, which lead to a ladder-like pattern after separation by size. Also in A20 B-lymphoma cells, incubation with FasL led to DNA laddering (Fig. 1C), and this effect was concentration dependent (data not shown). Pretreatment of cells with the caspase-3 inhibitor Ac-DEVD-cho or the broad-spectrum caspase inhibitor zVAD-fmk reduced DNA degradation or blocked it, respectively. By contrast, Ac-YVAD-cho did not protect A20 cells from Fas-induced DNA degradation (Fig. 1C). PS exposure on the cell surface was determined by flow fluorocytometric analysis of annexin-V-FITC binding. Appearance of PS on the cell surface, observed for about 80% of the cells after treatment with 100 ng/ml FasL for 5 hours, was inhibited by zVAD-fmk but not by Ac-DEVD-cho (Fig. 1D) or Ac-YVAD-cho (data not shown). Thus, by several criteria, caspase-3 was implicated in the execution of apoptosis in FasL-stimulated A20 cells; however, FasL-induced cell death could only be partially blocked by the caspase-3 inhibitor Ac-DEVD-cho, suggesting the existence of an alternative caspase-3-independent pathway leading to A20 cell death.

Ac-DEVD-cho treatment of A20 B-lymphoma cells revealed an alternative death signaling pathway originating from Fas

Cell viability after FasL treatment was investigated by an

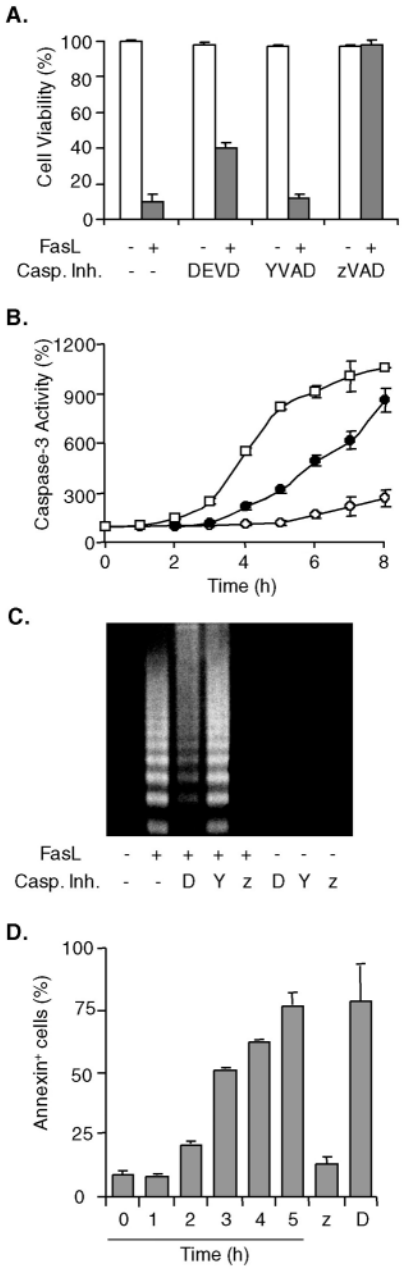

Fig. 1. Cell viability, caspase-3 activation, DNA fragmentation and surface exposure of phosphatidylserine in FasL-stimulated A20 B-lymphoma cells. (A) Cells were incubated for 30 minutes without (–) or with either 100 μM Ac-DEVD-cho (DEVD or D), 100 μM Ac-YVAD-cho (YVAD or Y) or 10 μM zVAD-fmk (zVAD or z). Then, cells were incubated for another 16 hours either without (white bars) or in the presence of 100 ng/ml of FasL (gray bars), and cell viability was determined by the MTS assay. (B) Caspase-3 activity was determined using the substrate Ac-DEVD-amc after incubation of cells (0-8 hours) with 10 (open circles), 32 (filled circles) or 100 (open squares) ng/ml FasL. (C) Cells were treated as described in (A), and after 4 hours of incubation with FasL, DNA fragmentation was analyzed by electrophoresis in agarose gels. (D) A20 cells were incubated (0 to 5 hours) with 100 ng/ml of FasL alone or 3 hours with FasL following pre-incubation with the inhibitor Ac-DEVD-cho (D) or zVAD-fmk (z), and then phosphatidylserine exposure on the cell surface was detected using Annexin-V-FITC. Only PI-negative cells, which represented approximately 90% of the total cell population, are shown. Data shown are the means with standard deviations from (A,B,D) or results representative of (C) three independent experiments.

alternative method using propidium iodide (PI), which labels DNA and permits the detection of cells that have lost their membrane integrity (Hetz et al., 2002). In the absence of FasL, no or little A20 cell death was detectable and, as a consequence, cells were only poorly PI positive (Fig. 2A, NT). Upon addition of 100 ng/ml FasL (Fig. 2A, FasL), an increase in staining was visible for a majority (90%) of the cells, corresponding to the population found previously to be non-viable (Fig. 1A). Surprisingly, the dead cell population was heterogeneous, being composed of hypodiploid (M1) and normodiploid (M2) cells. In the presence of Ac-DEVD-cho, only the hypodiploid population was reduced, whereas with zVAD-fmk, cell viability in general was maintained and neither dead cell population was detectable (Fig. 2A, DEVD+FasL and zVAD+FasL, respectively). Quantification of several such experiments (Fig. 2B) showed that upon FasL treatment roughly 60% of the dead cells were hypodiploid, whereas the remaining 30% possessed normal DNA content. Ac-DEVD-cho reduced the hypodiploid population from 60 to 35% but had no effect on dead cells with normal DNA content. Ac-YVAD-cho had no effect at the same concentration on either dead cell population observed in response to FasL, whereas zVAD-fmk eliminated both.

PI binding was also analyzed in permeabilized cells, where hypodiploid (apoptotic) cells were readily distinguishable from the rest (Fig. 2C). Addition of FasL (100 ng/ml) increased the hypodiploid population by 50%. This increase was substantially reduced by Ac-DEVD-cho and completely eliminated by zVAD-fmk. Taken together, these results suggested that FasL triggered apoptotic cell death in A20 cells via a caspase-3-dependent mechanism. However, a significant fraction of the cells (about 30%) died in a distinct fashion, requiring initiator caspases but not caspase-3 activation and occurring in the absence of characteristics of apoptosis.

Morphological analysis of cells treated with FasL

To further characterize this alternative Fas-mediated pathway, cell death observed in A20 cells in response to treatment with 100 ng/ml FasL for 16 hours was also characterized by electron microscopy (Fig. 3A-C). Predominantly two cell populations were detectable in response to FasL (Fig. 3B,C). In one population, signs of apoptosis, such as nuclear fragmentation, chromatin condensation and membrane blebbing were observed (Fig. 3B), whereas the other was characterized by the presence of disrupted nuclei and many vacuolar structures (Fig. 3C). In addition, the nuclear and cellular morphology after 16 hours of treatment with FasL were analyzed. Nuclear morphology was revealed by PI fluorescence using confocal microscopy (Fig. 3D). Upon treatment with FasL (100 ng/ml), 58±10% shrunken dead cells with condensed chromatin and a 1.5-fold reduced cell volume (A: apoptotic cells) were visible. FACS analysis following PI staining confirmed that the hypodiploid cell population was indeed smaller than non-treated cells (data not shown). Additionally, FasL induced approximately 37±8% swollen dead cells with normal nuclear

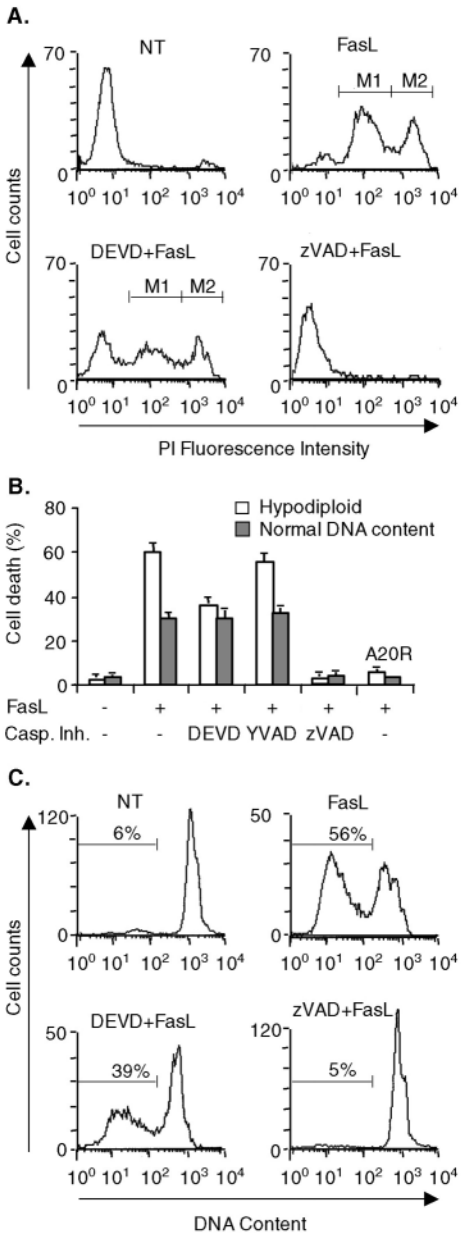

Fig. 2. FasL induced both apoptotic and necrotic cell death in A20 B-lymphoma cells. Cells were incubated for 30 minutes with or without 100 μM Ac-DEVD-cho (DEVD) or 10 μM zVAD-fmk (zVAD). Then FasL was added to a final concentration of 100 ng/ml, and cells were incubated for another 16 hours. Subsequently, cells were stained with PI, and cell survival was determined by flow cytometric analysis. (A) In response to FasL, two populations of PI-positive, dead cells, indicated as M1 (hypodiploid population) and M2 (dead cells with intact DNA), were distinguishable. (B) Statistical analysis of results from experiments as indicated in A, showing the means with standard deviation of three independent experiments. As additional negative controls, results obtained with cells resistant to FasL (A20R) are also shown. (C) In parallel, cells analyzed as in A were permeabilized with methanol and stained with PI to quantify total DNA content. Data shown are representative of three independent experiments with similar outcomes.

staining and a roughly three-fold increased cell volume. This second type of FasL-induced cell death is referred to from here on as necrosis (N, necrotic cells).

To confirm that the two populations of dead cells identified by FACS analysis (Fig. 2A) corresponded to apoptotic and necrotic cells, both dead cell populations were isolated by FACS cell sorting and then characterized by confocal microscopy. As expected, apoptotic and necrotic populations were highly enriched in cells with either condensed, fragmented DNA or normal nuclear morphology, respectively (Fig. 3E). Taken together, the data demonstrate that apoptotic and necrotic cell death occurred in response to FasL treatment in A20 cells and that the resulting two cell populations could be easily identified and quantified by FACS analysis.

A question arising at this point was whether a homogeneous A20 cell population was responding in two different ways to FasL or whether the behavior of two distinct A20 cell subpopulations was being analyzed: one that died via apoptosis and a second that died by necrosis. To address this issue, several clones (n=6) were isolated from the parent population by serial dilution and subsequently tested for their response to FasL (100 ng/ml). For all clones exactly the same pattern of cell death was observed as documented for the parent cell population (Fig. 2A,B), namely roughly 60% apoptosis versus 30% necrosis (data not shown). Thus, the A20 cells characterized here represent a homogeneous cell population that respond to FasL in two biochemically and morphologically distinguishable ways.

In situ caspase-3 and caspase-8 activity in FasL-treated A20 cells

Apoptosis is generally accompanied by a reduction in cell volume. Thus, this parameter was employed to discriminate between apoptotic and necrotic cells (Fig. 4A) and determine caspase activity in situ at time points when cell viability was still preserved (Fig. 4B). In addition, the subpopulations were isolated by FACS sorting and characterized in terms of their nuclear morphology (Fig. 4C) and evidence for DNA fragmentation (Fig. 4D). Cell-permeable fluorogenic substrates, which become fluorescent upon cleavage by caspases, were employed for caspase-3 (FAM-DEVD-fmk) and caspase-8 (FAM-LETD-fmk) activity. Treatment of A20 cells with FasL for 4 hours led to cell shrinkage (Fig. 4A, region R2), which was accompanied by caspase-3 activation (Fig. 4B) in approximately 65% of cells. No caspase-3 activation was detected in the remaining population (Fig. 4B, region R1). Interestingly, caspase-8 activity was detected in both populations of cells (Fig. 4B, R1 and R2) and was completely blocked by the pre-treatment with 5 μM of zVAD-fmk (data not shown). Furthermore, in the analysis of the nuclear morphology after FACS cell sorting of the cell population with reduced cell volume (R2), in which caspase-3 activation was observed, nuclear condensation and fragmentation (Fig. 4C, R2) were detected, although this was not the case for the rest of the cells that died by necrosis (Fig. 4C, R1). Electrophoretic analysis of DNA (Fig. 4D), isolated from the two subpopulations (R1 and R2), revealed DNA fragmentation, akin to that observed for the entire population (F), only in the R2 but not in the R1 subpopulation.

Comparative analysis of Fas-induced cell death in A20 B-, Jurkat T- and Raji B-cells

To increase the relevance of these observations described for A20 cells, additional models were sought. Jurkat T-cells and Raji B-cells were selected because of their susceptibility to Fas-dependent apoptosis. The ability of FasL (A20, Jurkat) or anti-Fas antibodies (Raji) to induce apoptosis and/or necrosis was assessed at different concentrations (Fig. 5A). Both apoptosis and necrosis were found to occur side-by-side at even the lowest concentrations of FasL tested and increased up to concentrations of roughly 100 ng/ml in A20 B- and Jurkat T-cells. Thereafter, as FasL concentrations increased further, a decline in necrosis was detectable. For A20 B- and Jurkat T-cells, results similar to those illustrated for FasL were also obtained using the anti-Fas antibody (data not shown), while the same treatment of Raji B-cells triggered a concentration-dependent increase in apoptosis only (Fig. 5A). Interestingly, very low concentrations of zVAD up to 1 μM selectively reduced Fas-induced apoptosis without affecting necrosis in both A20 and Jurkat cells (Fig. 5B). Taken together, these results suggest that Fas-dependent activation of initiator caspases above a threshold value may be necessary to trigger caspase-3 dependent apoptosis. For Jurkat cells, as previously shown with A20 cells (Fig. 4), activation of caspase-3 only occurred in cells of reduced volume (apoptosis), whereas caspase-8 activation was essentially detectable in all cells (data not shown). Thus, caspase-8 activation was a generic event occurring downstream of Fas in A20 and Jurkat cells, whereas caspase-3 activation was only observed in the subset of cells committed to apoptosis.

Ceramide generation after FasL stimulation

Previous reports have shown that, upon Fas ligation, lipid second messengers like ceramides are produced in lymphoid cells owing to the hydrolysis of plasma membrane sphingomyelin as a consequence of lipid scrambling (Brenner et al., 1997; Cock et al., 1998; Tepper et al., 1997; Tepper et al., 2000; Tepper et al., 2001). This phenomenon is reflected in PS exposure on the cell surface. Interestingly, we found that PS externalization occurred in both apoptotic and necrotic cells as evidenced by elimination of Annexin-V staining on most FasL-treated A20 cells in the presence of zVAD (Fig. 1D). Similar results were also obtained with A20 and Jurkat T cells in experiments analyzing the apoptotic and necrotic cell populations by FACS and comparing Annexin-V staining versus cell volume following FasL treatment. PS exposure was detected in both populations of cells. As predicted from the literature, no Annexin-V

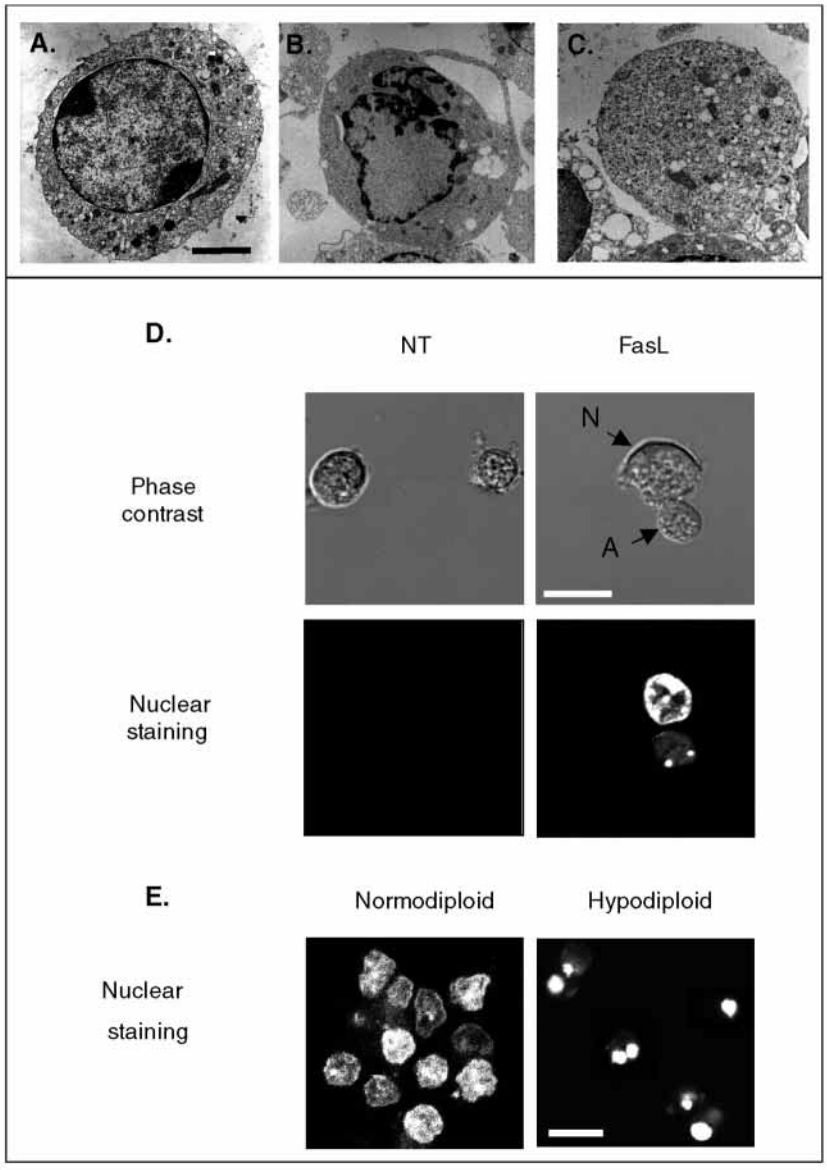

Fig. 3. Morphological analysis and DNA staining of A20 B-lymphoma cells treated with FasL. Untreated cells (A) or cells treated with 100 ng/ml FasL (B,C) for 16 hours were analyzed by electron microscopy. Necrotic FasL-treated cells (C) were characterized by disruption of the nuclei and abundance of vacuolar structures, whereas apoptotic cells observed in response to FasL were characterized by nuclear fragmentation, strong condensation of chromatin and membrane blebbing (B). The black bar shown for untreated cells (A) is equivalent to 5 μm. All images are shown at the same magnification. Alternatively, cells were left untreated (NT) or incubated with 100 ng/ml FasL for 16 hours, stained with PI and analyzed by confocal microscopy (D). As a comparison, non-treated cells are shown. Non-treated cells permeabilized with methanol (NT, Met-OH) and stained with PI (control, permeabilized) are shown as controls in Fig. 8A at the same magnification. Necrotic nuclei were PI positive, but retained a normal structural appearance (N); apoptotic nuclei were characterized by strong condensation of chromatin (A). Phase contrast and fluorescence images from the same optical section are shown. (E) Alternatively, hypodipliod and normodiploid cells were separated by FACS using PI fluorescence intensity as a parameter and analyzed subsequently by confocal microscopy (D). Images are shown at similar magnification. The bar in white is equivalent to 13 μm.

staining was detectable for Raji cells following Fas ligation (Fig. 5C).

Intriguingly, results in Fig. 5 indicated that Fas-induced necrosis may be linked to lipid scrambling and PS exposure because such events do not occur in Raji B-cells. Thus, levels of the lipid second messenger ceramide were measured in A20 cells using the diacylglycerol kinase assay (Preiss et al., 1987; Walsh and Bell, 1986). Upon treatment of A20 cells with FasL, ceramide levels increased noticeably and were at least two-fold above basal levels after 8 hours, whereas no such changes were detected in diacylglycerol levels (Fig. 6A). No significant changes in ceramide levels were detectable within the first hour of stimulation when A20 was compared with FasL-insensitive A20R cells (data not shown). Fluctuations in ceramide levels observed at the 3 hour time point were often within the range of fluctuations observed in A20R cells. On average (n=6 or more determinations), FasL treatment increased ceramide levels to 132±28 and 212±47 percent of baseline values, after 3 hours and 8 hours, respectively (Fig. 6B). Moreover, the kinetics of ceramide release described here were similar to those previously reported in response to Fas activation for Jurkat T-cells and U937 promyelocytic leukemia cells (Sillence and Allan, 1997; Tepper et al., 1997; Tepper et al., 2000). Thus, Fas-induced necrosis was observed in A20 and Jurkat cells where lipid scrambling, PS exposure and delayed ceramide increases occurred, but not in Raji cells lacking such events.

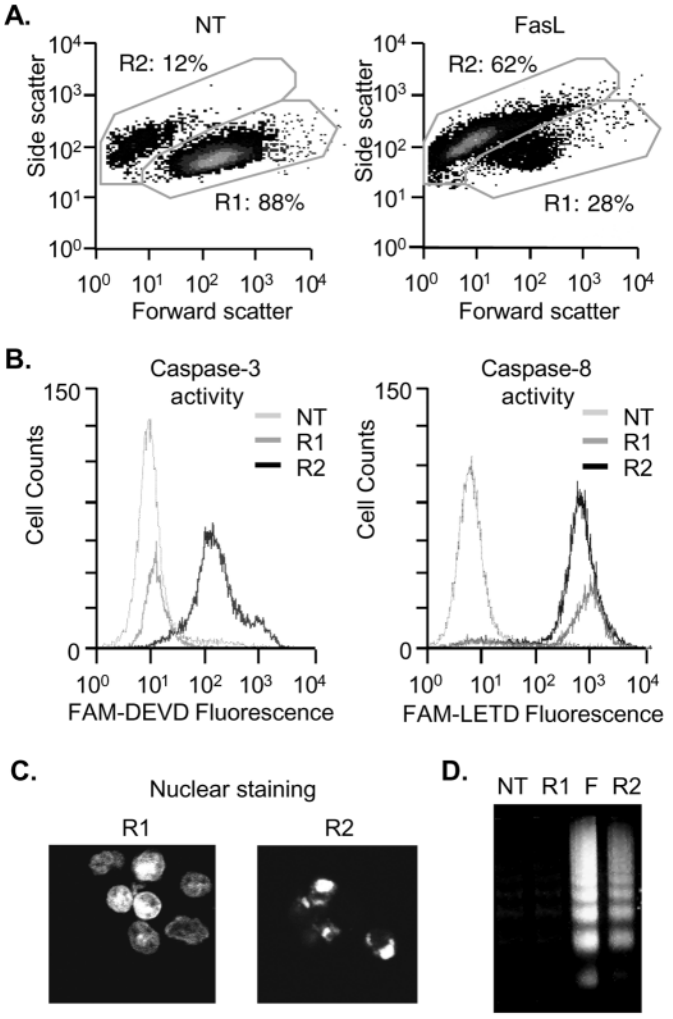

Fig. 4. Caspase-3 and caspase-8 activity in FasL-stimulated A20 B-lymphoma cells. (A) Cells were incubated for 4 hours either without (NT) or in the presence of 100 ng/ml of FasL (FasL), and cell volumes were determined by FACS analysis by plotting forward scatter versus side scatter. After treatment with FasL, approximately 65% of cells showed a reduction in cell volume (Region 2, R2). This phenomenon was not observed in non-treated cells (Region 1, R1). (B) Caspase-3 and caspase-8 activity in situ were determined by flow cytometric analysis using the cell permeable substrates FAM-DEVD-fmk and FAM-LETD-fmk, respectively. Non-treated cells (dotted line), or cells treated with 100 ng/ml FasL from regions R1 (grey line) and R2 (black line) region, are shown. Alternatively, both cell populations R1 and R2 were separated by cell sorting. Then, either nuclear morphology was analyzed by confocal microscopy following permeabilization with methanol and PI staining (C) or DNA fragmentation was visualized following electrophoresis in agarose gels (D). In the latter experiments, cells treated with 100 ng/ml FasL (F) or left untreated (NT) served as controls. Results shown are representative of two independent experiments performed in duplicates.

Cell-permeable C2- and C6-ceramides, but not the corresponding dihydro-ceramides, induced non-apoptotic death of A20 B-lymphoma cells

Intracellular release of ceramide upon FasL stimulation was detected either concomitantly with or after caspase-3 activation and onset of DNA fragmentation, suggesting that ceramide was unlikely to be mediating apoptosis. To evaluate whether and how ceramide might contribute to cell death, A20 cells were treated with the cell-permeable ceramide analogues N-acetyl- (C2-ceramide) and N-hexanoyl-sphingosine (C6-ceramide). C6-ceramide treatment for 16 hours reduced A20 viability in a concentration-dependent manner, whereas dihydro-C6-ceramide (DH-C6-ceramide) had no such effect (Fig. 7A). DH-C6-ceramide is similar to C6-ceramide but lacks a critical 4-trans double bond in the sphingosine backbone that is linked to biological activity of ceramides. Similar reductions in cell viability were also observed upon cell treatment with C2-ceramide, whereas DH-C2-ceramide had no effect (data not shown). Also, incubation of A20 B-lymphoma cells with 100 μM dioctanoylglycerol, a short-chain cell-permeable diacylglycerol analog, did not affect A20 cell viability (data not shown). Analysis of cell viability after C2 and C6-ceramide treatment by the PI exclusion method revealed that cells died with no or little alteration in DNA content as assessed both by DNA laddering (Fig. 7C) and flow cytometric analysis (Fig. 7D,E), suggesting that cell death occurred predominantly by necrosis. In agreement with this interpretation, cell death induced by cell-permeable ceramides was not associated with caspase-3 activation (Fig. 7B) and was not inhibited by Ac-DEVD-cho, Ac-YVAD-cho or zVAD-fmk (data not shown). Similar observations were also made in the presence of brain ceramides (predominantly C18-ceramides), although higher concentrations around 200 μM were required to reduce cell viability by 50% (data not shown). Likewise, necrosis was observed for different human B-lymphoma cell lines (Raji, Ramos, Daudi and M12), EBV-transformed human B-lymphoblast cells (GES and LM) as well as Jurkat cells upon treatment with cell-permeable ceramides (data not shown and Fig. 7E).

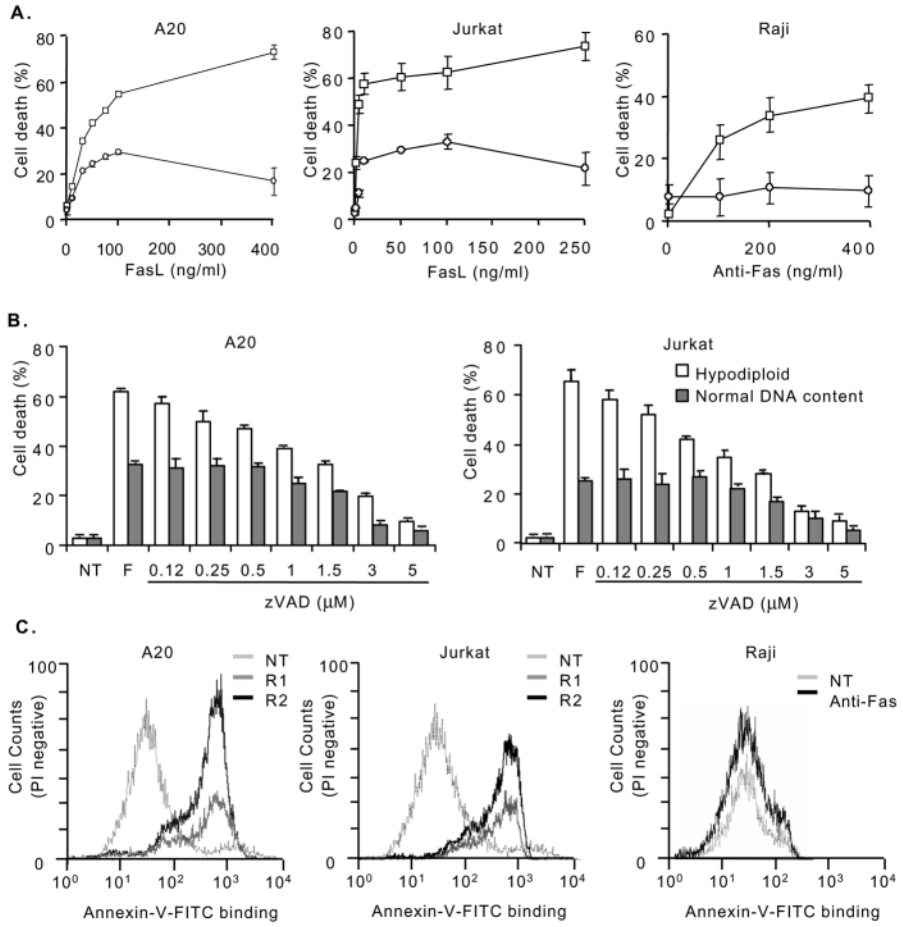

Fig. 5. Comparison of FasL-induced cell death in A20, Jurkat and Raji cells. (A) Cells were incubated either with increasing concentrations up to 400 ng/ml of FasL (A20, Jurkat cells) or up to 400 ng/ml of anti-Fas antibody (Raji cells) for 16 hours, stained with PI and cell death was assessed. (B) A20 and Jurkat cells were incubated with or without (NT) 100 ng/ml FasL after pre-treatment for 30 minutes with the indicated low concentrations (0-5 μM) of zVAD-fmk (zVAD). Cell death was quantified by flow cytometric analysis (see Fig. 2). Squares or empty bars indicate the percentage of apoptotic cells, and circles or gray bars indicate necrotic cells (A,B). Results averaged from three experiments are shown. Also, PS exposure on the cell surface of A20, Jurkat and Raji cells was detected by FACS using Annexin-V-FITC 5 hours following Fas activation (C). Subpopulations R1 and R2 indicated for A20 and Jurkat cells were obtained as described in Fig. 4. Results shown are representative of two independent experiments.

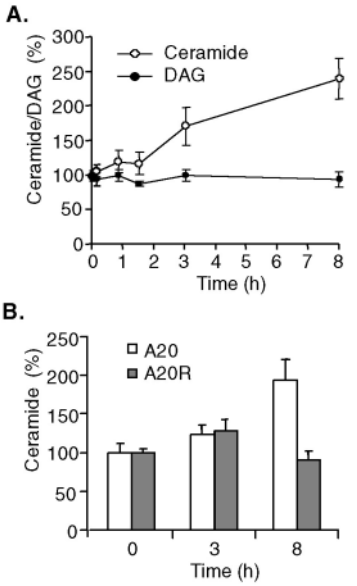

Fig. 6. Ceramide and diacylglycerol levels in FasL-stimulated A20 and A20R cells. After addition of 100 ng/ml FasL, A20 or A20R cells were incubated for the indicated time periods at 37°C. Lipids were extracted and analyzed using the diacylglycerol kinase assay and expressed as a percentage of basal levels. (A) Ceramide (open circles) and diacylglycerol (filled circles) levels 0-8 hours after FasL stimulation are shown in A20 cells. (B) Comparison in A20 and A20R cells of ceramide levels at the time points 3-8 hours following FasL addition. Results shown (means with standard deviation) were either from an individual experiment done in triplicate in which ceramide levels were already visibly elevated after 3 hours (A) or were averaged from two or more independent experiments done in triplicate for each time point.

Modification of endogenous ceramide levels by treatment with bacterial SMase

To further analyze the role of ceramide in Fas-induced cell death, endogenous ceramide levels were increased by treating cells with the recombinant *Staphylococcus aureus* SMase. Such treatment of A20 cells increased cellular ceramide levels (data not shown) and reduced cell viability in a dose-dependent fashion (Fig. 7F). Interestingly, analysis of PI uptake and DNA content (Fig. 7G) suggested that cells died predominantly by necrosis. As expected, A20 cell death triggered by bacterial SMase occurred in the absence of caspase-3 activation (data not shown). In conclusion, Fas-induced apoptosis and ceramide-induced cell death were distinct events in A20, Jurkat and Raji cells; however, necrosis observed in response to FasL resembled cell death triggered by the cell-permeable C2- and C6-ceramide analogs, brain-ceramides or treatment with bacterial SMase.

FasL-induced caspase-3 activation, cell shrinkage and onset of DNA fragmentation were apparent within the first 2-3 hours of FasL (100 ng/ml) addition. Significantly, elevated ceramide levels, however, were observed at later time points. This raised the possibility that intracellular ceramide production may serve as a mechanism permitting A20 cells to die by necrosis in cells where caspase-3 activation either did not occur or was insufficient to trigger apoptosis. In agreement with this hypothesis, concomitant addition of C2-ceramide with FasL resulted almost exclusively in necrotic cell death after 16 hours (Fig. 8A). As ceramide addition was delayed, the ratio of apoptotic to necrotic cell death became increasingly reminiscent of the pattern observed with FasL alone (Fig. 8A),

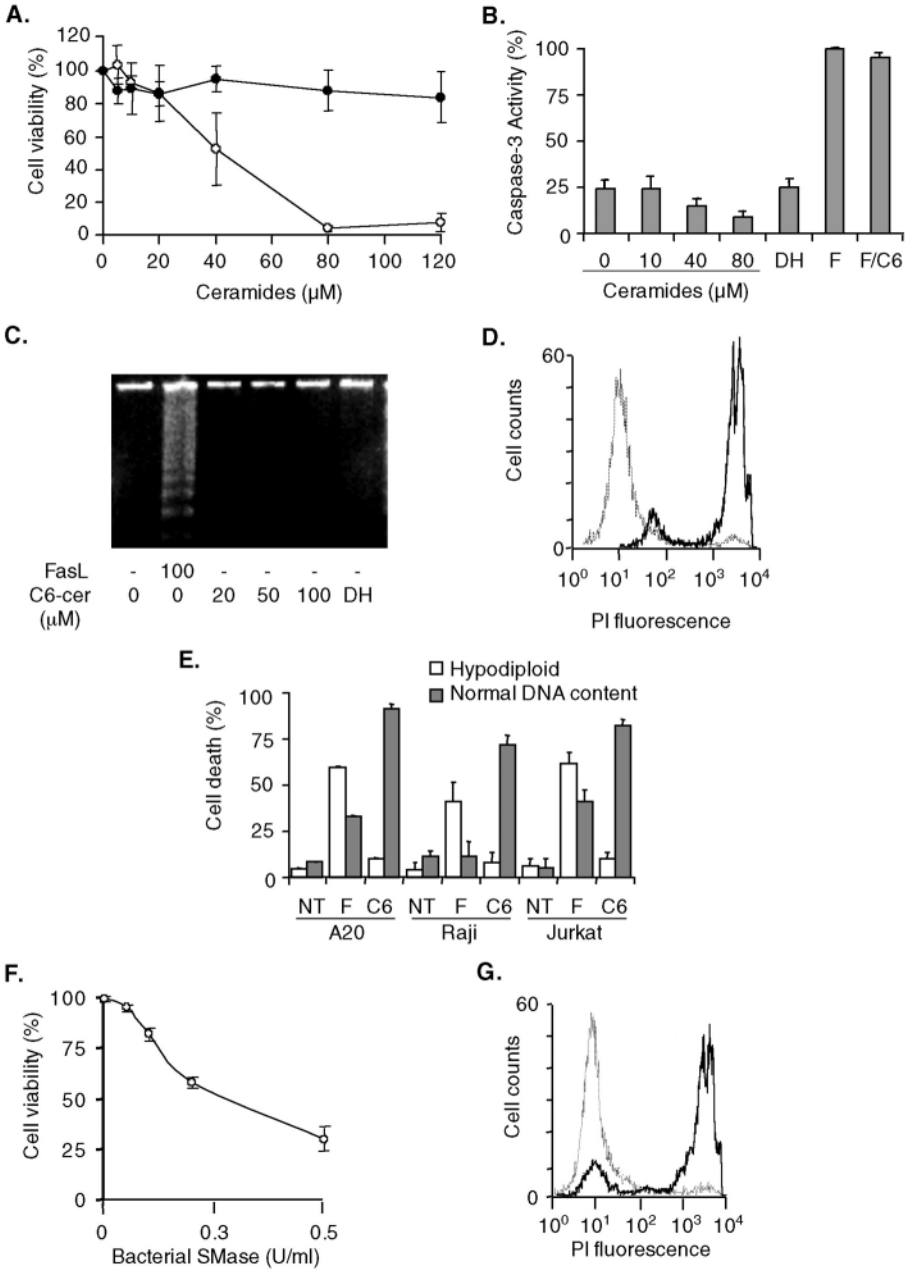

Fig. 7. Cell-permeable ceramides or treatment with bacterial SMase induced death by a caspase-3-independent mechanism. (A) A20 cells were incubated for 16 hours with 0-120 μM C6-ceramide (open circles) or dihydro-C6-ceramide (closed circles). Cell viability was determined by the MTS assay and expressed as percentage of cell viability observed for non-treated cells. (B) Caspase-3 activity was determined after treatment of A20 cells for 4 hours either with C6-ceramide at the concentrations indicated, with 80 μM dihydro-C6-ceramide (DH), with 100 ng/ml FasL (F), with 100 ng/ml FasL and 80 μM C6-ceramide (F/C6) or remained untreated. Values are shown as a percentage of the caspase-3 activity in the presence of 100 ng/ml FasL alone. (C) Alternatively, DNA fragmentation was analyzed by electrophoresis in agarose gels after treatment with FasL or different concentration of ceramides for 4 hours. (D) A representative experiment is shown where A20 cells were treated with 100 μM C6- (black) or dihydro-C6 (gray) ceramide for 16 hours and cell survival was determined by flow-cytometric analysis following PI staining. (E) A20, Jurkat and Raji cells were either not treated (NT) or treated with 100 μM C6-ceramides (C6) or 100 ng/ml FasL (F) for 16 hours. Then cells were harvested, stained with PI and cell survival was determined by flow cytometric analysis. (F) Cells were treated with bacterial SMase at the concentrations indicated for 16 hours and cell viability was determined by the MTS assay. (G) In parallel, cells either not treated (gray) or treated with 0.5 U/ml bacterial SMase (black) were stained with PI, and cell survival was determined by flow cytometric analysis. The results shown are either the means or standard deviations of three independent experiments (A,B,E,F) or are representative of at least three independent experiments (C,D,G).

suggesting that the time point at which ceramide levels were elevated in this experimental system may serve to define the ultimate nature of cell death observed. Quite remarkably, simultaneous addition of C6-ceramide and FasL did not prevent caspase-3 activation (Fig. 7C), indicating that ceramide promoted events lying on a pathway parallel to caspase-3 activation. Similar results were also obtained with Jurkat T-cells (data not shown). Taken together these observations suggest that Fas-dependent elevation of endogenous ceramide in A20 and Jurkat cells may be delayed in order to induce necrosis only in those cells not committed to apoptosis via caspase-3 activation. Interestingly, the addition of cell-permeable ceramides to Raji cells 4-6 hours after triggering Fas also no longer altered the degree of apoptosis detected (Fig. 8B). The elevated levels of necrosis observed in this case reflect the fact that only about 50% of the Raji cells died upon Fas ligation (see Fig. 5A), suggesting that Raji cells not committed to death via Fas remained sensitive to ceramide. Thus, in all three lines characterized, cell-permeable ceramides only altered the apoptotic fate of Fas-stimulated cells when added within the first 4-6 hours following Fas activation.

Morphological analysis of cells treated with cell permeable ceramide

The nuclear and cellular morphology after C2-ceramide treatment were determined in A20 cells (Fig. 9). Nuclear morphology of dead cells was revealed by PI fluorescence using confocal microscopy after 16 hours of treatment (Fig. 9A). In cells treated with C2-ceramide neither chromatin condensation nor cell shrinkage were observed. Instead, ceramide-induced dead cells were two- to three-fold larger than

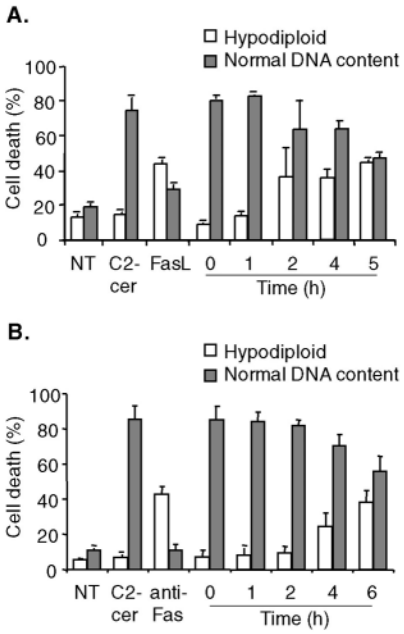

Fig. 8. Effect of cell permeable ceramides on FasL-induced cell death. (A) A20 or Raji cells (B) cells were incubated with 100 ng/ml FasL and C2-ceramide (100 μM) was added at time different time points after FasL. For comparison, cells were either not treated (NT or incubated with C2-ceramide (100 μM) or FasL (A20) or anti-Fas (Raji) (100 ng/ml) alone. For analysis, cells were harvested after 16 hours, stained with PI, and cell survival was determined by flow cytometric analysis (see Fig. 2). Means and standard deviations of data from three independent experiments are shown.

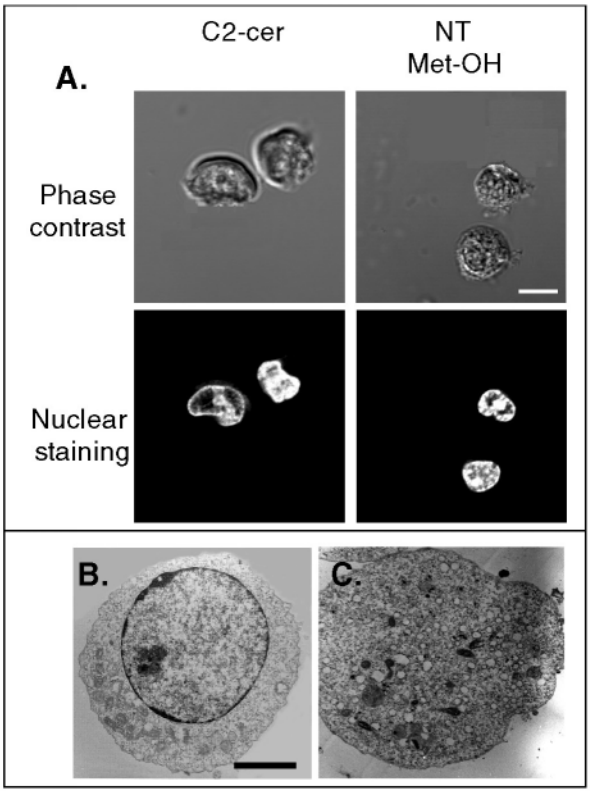

Fig. 9. Morphological analysis and DNA staining of A20 B-lymphoma cells treated with cell-permeable ceramides. (A) Cells were incubated with 100 μM C2-ceramide for 16 hours, stained with PI and analyzed by confocal microscopy. As a comparison, non-treated cells were permeabilized with methanol (NT, Met-OH) and stained with PI (control, permeabilized). Phase contrast and fluorescence images from the same optical section are shown. The bar shown in white is equivalent to 13 μm. All images are shown at the same magnification. Alternatively, cells untreated (B) or treated with 100 μM C2-ceramide (C) for 16 hours were analyzed by electron microscopy. Necrotic C2-ceramide- (C) treated cells were both characterized by disruption of the nuclei and abundance of vacuolar structures. The black bar shown for untreated cells (B) is equivalent to 5 μm. The image in panel C is shown at the same magnification.

untreated cells. Cell death observed in A20 cells in response to treatment with 100 μM C2-ceramide for 16 hours was also characterized by electron microscopy (Fig. 9B,C). In perfect agreement with our other results, cells treated with C2-ceramide (Fig. 9C) resembled very strongly the necrotic cell population (Fig. 3C) observed in response to FasL treatment. Thus, by the criteria investigated, ceramide-induced death strongly resembled FasL-induced necrosis.

Discussion

Several crucial events linked to onset of apoptosis in A20 cells, including caspase-3 activation, cell shrinkage and DNA fragmentation, were all activated within the first 3 hours of FasL addition. However, cell viability was only partially restored in the presence of the caspase-3 inhibitor Ac-DEVD-cho, whereas a more general caspase inhibitor, zVAD-fmk, completely protected cells against FasL-induced death (Fig. 1). Flow cytometric analysis distinguished two PI-positive cell populations in which cell death was either caspase-3-dependent and paralleled by DNA fragmentation or caspase-3- and DNA fragmentation-independent (Fig. 2). By morphological criteria (Fig. 3), these two subpopulations were identified as apoptotic and necrotic cells, respectively. Furthermore, FACS analysis showed that caspase-3 activation only occurred in the shrunken cell population (apoptosis), whereas caspase-8 activation was detectable in both (Fig. 4). Thus, activation of initiator caspases, such as caspase-8, represented a key initial step triggered by FasL leading to apoptotic and necrotic death in A20 cells. Activation of caspase-3, by contrast, was only implicated in events leading to apoptosis. Interestingly, similar effects were also observed in Jurkat T cells, whereas in Raji B-cells lacking PS externalization and delayed ceramide production (Tepper et al., 2000) only Fas-induced apoptosis was observed (Fig. 5).

The initiation of signaling pathways via Fas that lead to both apoptotic and necrotic cell death has been described in some experimental systems. In murine L929 fibrosarcoma cells, necrosis was observed downstream of Fas when caspase activation was blocked by inhibitors (Vercammen et al., 1998a). Also, caspase inhibition rendered murine L929 fibrosarcoma cells 1000-fold more sensitive to necrosis induced by TNF-α (Vercammen et al., 1998b). FasL-induced necrosis in the absence of caspase activation owing to activation of receptor-interacting protein (RIP) has also been described previously (Holler et al., 2000). These results suggest that necrosis is either favored when pathways normally

leading to apoptosis are blocked or when an alternative, caspase-independent pathway is triggered. Our results extend such observations by showing that apoptosis and necrosis require caspase activation and may be triggered in the absence of caspase inhibitors. In fact, low concentrations of zVAD (less than 1 μM) were employed to selectively reduce Fas-induced apoptosis without modulating necrosis, whereas at higher concentrations both modes of cell death are reduced (Fig. 5B). Thus, elevated levels of initiator caspase-8 activity appear to favor FasL-induced apoptosis and, as a pre-requisite, caspase-3 activation.

Analysis of ceramide levels after Fas stimulation revealed minor fluctuations at early time points (up to 3 hours). However, the intracellular ceramide concentrations doubled on average roughly 8 hours after stimulation with FasL (Fig. 6A,B). Our observations in A20 cells are consistent with previous results showing that Fas-induced apoptosis of lymphoid cells is accompanied by a late phase of caspase-dependent ceramide production (Sillence and Allan, 1997; Tepper et al., 1997), coinciding temporally with events occurring after caspase-3 activation, such as nuclear fragmentation.

Recently, caspase-8-dependent but caspase-3-independent lipid scrambling and late production of ceramide have been reported in Jurkat T cells. Neither of these changes were detected in Raji B-cells in response to Fas activation (Tepper et al., 2000). Our results identified A20 B-cells as being similar to Jurkat T cells in three ways: first, PS externalization was detectable in essentially all A20 cells committed to death (apoptotic and necrotic cells) within the first 5 hours after addition of FasL (Fig. 5C) and was blocked with low concentrations of zVAD-fmk but not with caspase-3 inhibitors (Fig. 1D). Second, delayed ceramide production with similar release kinetics was detectable (Fig. 6) (Tepper et al., 2000). Third, in both lines FasL triggered apoptosis and necrosis, albeit in a distinct fashion with respect to their concentration dependence (Fig. 5). Raji B-cells, in contrast, only died by apoptosis (Fig. 5). Thus, our observations, in conjunction with previously published results (Tepper et al., 2000), provide a link between Fas-induced lipid scrambling, late ceramide production and cell death by necrosis.

Delayed ceramide production was additionally linked to FasL-induced necrosis since cell-permeable C6- or C2-ceramide induced cell death ($LD_{50} \cong 40$ μM after 16 hours) without caspase-3 activation, DNA fragmentation, cell shrinkage and chromatin condensation (Figs 7 and 9). Instead, cells increased in size (Fig. 9A) and were filled with vacuolar structures (Fig. 9C), resembling FasL-induced cell death by necrosis (see Fig. 3C-E). Likewise, increases in endogenous ceramide levels upon treatment with bacterial SMase also promoted cell death by necrosis (Fig. 7F,G). Experiments in which ceramides were added to A20 cells at different time points after stimulation with FasL identified the ceramide-effect as being dominant in the sense that the earlier ceramide was present, the higher the percentage of cell death via necrosis. However, once the apoptotic program had been initiated, exogenous addition of ceramides no longer had any effect, and execution of apoptosis proceeded normally (Fig. 8A). Interestingly, similar effects were observed for Jurkat (not shown) and Raji cells (Fig. 8B), indicating that the kinetics of events leading to apoptosis were well conserved between cell lines and that delayed elevation of ceramide by exogenous supplementation had remarkably similar consequences.

Sphingomyelin, initially located in the outer leaflet of the plasma membrane, accumulates in the inner leaflet as a consequence of lipid scrambling, and this is reflected in PS externalization. Hydrolysis in the inner leaflet by a neutral SMase is then held responsible for late ceramide production (Tepper et al., 2000). For Raji B-cells lacking lipid-scrambling activity, ceramide levels do not increase in response to Fas activation and, as a consequence, substrate availability is proposed to represent a rate limiting step in activation of the neutral SMase responsible (Tepper et al., 2000). Raji cells, unlike A20 B- and Jurkat T-cells, did not undergo Fas-induced necrosis, supporting the notion that Fas-induced delayed ceramide increases promote necrosis. Consistent with this interpretation, addition of cell-permeable ceramides and treatment of cells with bacterial SMase triggered necrosis. However, experiments to implicate further one or the other intracellular pathway known to regulate ceramide levels were unsuccessful. In our hands, none of the compounds that reportedly modulate either neutral SMase [reduced glutathione, L-buthionine-[S,R]-sulfoximine: (Liu et al., 1998)) or acidic SMase (Imipramine: (Strelow et al., 2000)] activity or ceramide biosynthesis [Fumonisin B1: (Blazquez et al., 2000)] altered significantly Fas-induced necrosis (data not shown). Thus, our experiments have so far not provided a link at the molecular level to connect lipid scrambling, delayed ceramide increases and necrosis. Further experiments are needed to address such issues.

Several reports have suggested that ceramide production participates in apoptotic cell death, mainly by correlating the simultaneous appearance of apoptotic markers with ceramide production (Garcia-Ruiz et al., 1997; Gudz et al., 1997). However, experiments in which genetic manipulation was employed to analyze the contribution of different SMases in Fas-induced apoptosis failed to implicate any of these enzymes (Brenner et al., 1997; Cock et al., 1998; Tepper et al., 2001). In our experimental system, a small subpopulation of hypodiploid cells was observed by the FACS analysis after ceramide treatment (Fig. 7D). These most probably represent apoptotic cells. Others have reported induction of apoptosis in a small fraction of A20 cells (roughly 15%) by cell-permeable ceramide after 16 hours of incubation (Bras et al., 2000). The amount of necrosis induced by ceramide treatment appears to depend on the cell line investigated. For instance, in the human colon carcinoma cell line HT29, ceramide at 20 μM induces cell death in roughly 30% of the population and only about half of those cells die by apoptosis (C.A.H. and A.F.G.Q., unpublished). Since the assays generally employed are not quantitative and are heavily geared towards detecting apoptosis, it is conceivable that information concerning other forms of cell death might have gone largely unperceived.

In contrast to apoptosis, cell death by necrosis is typically associated with inflammation. This difference is related to activation or maturation of phagocytic cells, like macrophages and dendritic cells (Fadok et al., 2000; McDonald et al., 1999; Sauter et al., 2000). Recently, Bhardwaj and coworkers showed that immature dendritic cells phagocytose a variety of apoptotic and necrotic cells (Sauter et al., 2000). However, only exposure to necrotic cells provided the signals required for dendritic cell maturation, resulting in upregulation of

maturation-specific markers, co-stimulatory molecules and the capacity to induce antigen-specific $CD4^+$ and $CD8^+$ T-cells. Thus, dendritic cells are able to distinguish between the two types of dead cells and respond in a distinct manner. Although the interaction between apoptotic and phagocytic cells induces an anti-inflammatory response (Fadok et al., 2000), necrosis appears to be critical for initiation of an immune response (Holler et al., 2000; Sauter et al., 2000). Interestingly, the results presented here reinforce the notion that lipid scrambling and PS externalization do not provide the molecular basis to distinguish between cells dying by apoptosis or necrosis and, as a consequence, elicit different responses of the immune system.

Simultaneous or delayed activation of pathways leading to necrotic and apoptotic death in the same cells is likely to occur fairly frequently (Ankarcrona et al., 1995; Barros et al., 2001; Dypbukt et al., 1994; Hetz et al., 2002; Jonas et al., 1994). It has been proposed that the modification of intracellular ATP concentrations may serve as one possible mechanism permitting the switch from apoptotic to necrotic cell death (Leist et al., 1997). Indeed, ceramides have been shown to directly modulate mitochondria function, for instance, by inhibiting the mitochondrial respiratory complex III (Garcia-Ruiz et al., 1997; Gudz et al., 1997; Quillet-Mary et al., 1997). Thus, ceramide-induced necrosis may result from a decrease in ATP levels due to mitochondrial dysfunction. Consistent with this notion, a decrease in mitochondrial membrane potential was detected in A20 cells after at least one hour of incubation with cell permeable ceramides (data not shown). However, further experiments are required to determine how ceramide promotes necrosis in the cells characterized here.

In summary, the results presented show that two different pathways emerge from the Fas-receptor, one leading to caspase-3-dependent apoptosis and the other favoring necrosis in a manner dependent upon activation of caspase-8, but not execution caspases, like caspase-3. In addition, Fas-dependent, delayed production of ceramide was observed. The evidence available suggests that the time point at which ceramide levels were substantially elevated dictated the extent to which necrosis was observed. Thus, Fas-induced ceramide release is proposed to permit cells to undergo necrosis when caspase-8 activation occurred but was insufficient to trigger caspase-3-dependent apoptosis. Ceramide production in A20 B-cells and Jurkat T-cells downstream of caspase-8 may be temporally delayed to trigger necrosis only in those cells not already committed to apoptosis.

Salvatore Valitutti, Felipe Barros, Andres Stutzin, Bruno Antonsson are thanked for careful revision and thoughtful comments concerning the manuscript. Pascal Schneider and Jürg Tshopp are gratefully acknowledged for providing recombinant human FasL and polyADP-ribose polymerase antibodies, Cecilia Sepúlveda for use of the FACS machine and Nancy Olea for cell analysis by electron microscopy. Parts of these results have been presented previously in abstract form (Abstract#21, XV Annual Meeting of the Cell Biology Society of Chile, Valdivia, Nov. 2001). The paper is dedicated to Mrs. O.E. Quest who died of cancer while the work described was in progress.

References

Abbas, A. K. (1996). Die and let live: eliminating dangerous lymphocytes. *Cell* **84**, 655-657.

Ankarcrona, M., Dypbukt, J. M., Bonfoco, E., Zhivotovsky, B., Orrenius, S., Lipton, S. A. and Nicotera, P. (1995). Glutamate-induced neuronal death: a succession of necrosis or apoptosis depending on mitochondrial function. *Neuron* **15**, 961-973.

Barros, L. F., Stutzin, A., Calixto, A., Catalan, M., Castro, J., Hetz, C. and Hermosilla, T. (2001). Nonselective cation channels as effectors of free radical-induced rat liver cell necrosis. *Hepatology* **33**, 114-122.

Blazquez, C., Galve-Roperh, I. and Guzman, M. (2000). De novo-synthesized ceramide signals apoptosis in astrocytes via extracellular signal-regulated kinase. *FASEB J.* **14**, 2315-2322.

Boldin, M. P., Goncharov, T. M., Goltsev, Y. V. and Wallach, D. (1996). Involvement of MACH, a novel MORT1/FADD-interacting protease, in Fas/APO-1- and TNF receptor-induced cell death. *Cell* **85**, 803-815.

Bras, A., Albar, J. P., Leonardo, E., de Buitrago, G. G. and Martinez, A. C. (2000). Ceramide-induced cell death is independent of the Fas/Fas ligand pathway and is prevented by Nur77 overexpression in A20 B cells. *Cell Death Differ.* **7**, 262-271.

Brenner, B., Koppenhoefer, U., Weinstock, C., Linderkamp, O., Lang, F. and Gulbins, E. (1997). Fas- or ceramide-induced apoptosis is mediated by a Rac1-regulated activation of Jun N-terminal kinase/p38 kinases and GADD153. *J. Biol. Chem.* **272**, 22173-22181.

Cifone, M. G., Roncaioli, P., de Maria, R., Camarda, G., Santoni, A., Ruberti, G. and Testi, R. (1995). Multiple pathways originate at the Fas/APO-1 (CD95) receptor: sequential involvement of phosphatidylcholine-specific phospholipase C and acidic sphingomyelinase in the propagation of the apoptotic signal. *EMBO J.* **14**, 5859-5868.

Cock, J. G., Tepper, A. D., de Vries, E., van Blitterswijk, W. J. and Borst, J. (1998). CD95 (Fas/APO-1) induces ceramide formation and apoptosis in the absence of a functional acid sphingomyelinase. *J. Biol. Chem.* **273**, 7560-7565.

Cornall, R. J., Goodnow, C. C. and Cyster, J. G. (1995). The regulation of self-reactive B cells. *Curr. Opin. Immunol.* **7**, 804-811.

Dypbukt, J. M., Ankarcrona, M., Burkitt, M., Sjoholm, A., Strom, K., Orrenius, S. and Nicotera, P. (1994). Different prooxidant levels stimulate growth, trigger apoptosis, or produce necrosis of insulin-secreting RINm5F cells. The role of intracellular polyamines. *J. Biol. Chem.* **269**, 30553-30560.

Fadok, V. A., Bratton, D. L., Rose, D. M., Pearson, A., Ezekewitz, R. A. and Henson, P. M. (2000). A receptor for phosphatidylserine-specific clearance of apoptotic cells. *Nature* **405**, 85-90.

Garcia-Ruiz, C., Colell, A., Mari, M., Morales, A. and Fernandez-Checa, J. C. (1997). Direct effect of ceramide on the mitochondrial electron transport chain leads to generation of reactive oxygen species. Role of mitochondrial glutathione. *J. Biol. Chem.* **272**, 11369-11377.

Genestier, L., Prigent, A. F., Paillot, R., Quemeneur, L., Durand, I., Banchereau, J., Revillard, J. P. and Bonnefoy-Berard, N. (1998). Caspase-dependent ceramide production in Fas- and HLA class I-mediated peripheral T cell apoptosis. *J. Biol. Chem.* **273**, 5060-5066.

Gudz, T. I., Tserng, K. Y. and Hoppel, C. L. (1997). Direct inhibition of mitochondrial respiratory chain complex III by cell-permeable ceramide. *J. Biol. Chem.* **272**, 24154-24158.

Hahne, M., Renno, T., Schroeter, M., Irmler, M., French, L., Bornard, T., MacDonald, H. R. and Tschopp, J. (1996). Activated B cells express functional Fas ligand. *Eur. J. Immunol.* **26**, 721-724.

Hannun, Y. A., Obeid, L. M. and Dbaibo, G. S. (1996). Ceramide. A novel second messenger and lipid mediator. In *Handbook of Lipid Research*, vol. 8 (ed. R. M. Bell, J. H. Exton and S. M. Prescott), pp. 177-204. New York: Plenum Press.

Heinrich, M., Wickel, M., Schneider-Brachert, W., Sandberg, C., Gahr, J., Schwandner, R., Weber, T., Saftig, P., Peters, C., Brunner, J. et al. (1999). Cathepsin D targeted by acid sphingomyelinase-derived ceramides. *EMBO J.* **18**, 5252-5263.

Hetz, C., Bono, M. R., Barros, L. F. and Lagos, R. (2002). Microcin E492, a channel-forming bacteriocin from *Klebsiella pneumoniae*, induces apoptosis in some human cell lines. *Proc. Natl. Acad. Sci. USA* **99**, 2696-2701.

Hofmann, K. and Dixit, V. M. (1998). Ceramide in apoptosis–does it really matter? *Trends Biochem. Sci.* **23**, 374-377.

Holler, N., Zaru, R., Micheau, O., Thome, M., Attinger, A., Valitutti, S., Bodmer, J. L., Schneider, P., Seed, B. and Tschopp, J. (2000). Fas triggers an alternative, caspase-8-independent cell death pathway using the kinase RIP as effector molecule. *Nat. Immunol.* **1**, 489-495.

Jonas, D., Walev, I., Berger, T., Liebetrau, M., Palmer, M. and Bhakdi, S. (1994). Novel path to apoptosis: small transmembranes pores created by

staphylococcal alpha-toxin in T lymphocytes evoke internucleosomal DNA degradation. *Infect. Immun.* **62**, 1304-1312.

Kolesnick, R. N. and Kronke, M. (1998). Regulation of ceramide production and apoptosis. *Annu. Rev. Physiol.* **60**, 643-665.

Laster, S. M., Wood, J. G. and Gooding, L. R. (1988). Tumor necrosis factor can induce both apoptotic and necrotic cell lysis. *J. Immunol.* **141**, 2629-2634.

Leist, M., Single, B., Castoldi, A. F., Kuhnle, S. and Nicotera, P. (1997). Intracellular adenosine triphosphate (ATP) concentration: a switch in the decision between apoptosis and necrosis. *J. Exp. Med.* **185**, 1481-1486.

Liu, B., Andrieu-Abadie, N., Levade, T., Zhang, P., Obeid, L. M. and Hannun, Y. A. (1998). Glutathione regulation of neutral sphingomyelinase in tumor necrosis factor-alpha-induced cell death. *J. Biol. Chem.* **273**, 11313-11320.

Majno, G. and Joris, I. (1995). Apoptosis, oncosis, and necrosis. An overview of cell death. *Am. J. Pathol.* **146**, 3-15.

Martins, L. M. and Earnshaw, W. C. (1997). Apoptosis: alive and kicking in 1997. *Trends Cell Biol.* **7**, 111-114.

Matiba, B., Mariani, S. M. and Krammer, P. H. (1997). The CD95 system and the death of a lymphocyte. *Semin. Immunol.* **9**, 59-68.

McDonald, P. P., Fadok, V. A., Bratton, D. and Henson, P. M. (1999). Transcriptional and translational regulation of inflammatory mediator production by endogenous TGF-beta in macrophages that have ingested apoptotic cells. *J. Immunol.* **163**, 6164-6172.

Nagata, S. (1997). Apoptosis by death factor. *Cell* **88**, 355-365.

Nagata, S. and Golstein, P. (1995). The Fas death factor. *Science* **267**, 1451-1456.

Preiss, J. E., Loomis, C. R., Bell, R. M. and Niedel, J. E. (1987). Quantitative measurement of sn-1,2-diacylglycerols. *Methods Enzymol.* **141**, 294-300.

Quillet-Mary, A., Jaffrezou, J. P., Mansat, V., Bordier, C., Naval, J. and Laurent, G. (1997). Implication of mitochondrial hydrogen peroxide generation in ceramide-induced apoptosis. *J. Biol. Chem.* **272**, 21388-21395.

Rathmell, J. C. and Thompson, C. B. (1999). The central effectors of cell death in the immune system. *Annu. Rev. Immunol.* **17**, 781-828.

Sauter, B., Albert, M. L., Francisco, L., Larsson, M., Somersan, S. and Bhardwaj, N. (2000). Consequences of cell death: exposure to necrotic tumor cells, but not primary tissue cells or apoptotic cells, induces the maturation of immunostimulatory dendritic cells. *J. Exp. Med.* **191**, 423-433.

Sillence, D. J. and Allan, D. (1997). Evidence against an early signalling role for ceramide in Fas-mediated apoptosis. *Biochem. J.* **324**, 29-32.

Strelow, A., Bernardo, K., Adam-Klages, S., Linke, T., Sandhoff, K., Kronke, M. and Adam, D. (2000). Overexpression of acid ceramidase protects from tumor necrosis factor- induced cell death. *J. Exp. Med.* **192**, 601-612.

Suda, T., Takahashi, T., Golstein, P. and Nagata, S. (1993). Molecular cloning and expression of the Fas ligand, a novel member of the tumor necrosis factor family. *Cell* **75**, 1169-1178.

Tepper, A. D., Cock, J. G., de Vries, E., Borst, J. and van Blitterswijk, W. J. (1997). CD95/Fas-induced ceramide formation proceeds with slow kinetics and is not blocked by caspase-3/CPP32 inhibition. *J. Biol. Chem.* **272**, 24308-24312.

Tepper, A. D., Ruurs, P., Borst, J. and van Blitterswijk, W. J. (2001). Effect of overexpression of a neutral sphingomyelinase on CD95-induced ceramide production and apoptosis. *Biochem. Biophys. Res. Commun.* **280**, 634-639.

Tepper, A. D., Ruurs, P., Wiedmer, T., Sims, P. J., Borst, J. and van Blitterswijk, W. J. (2000). Sphingomyelin hydrolysis to ceramide during the execution phase of apoptosis results from phospholipid scrambling and alters cell-surface morphology. *J. Cell Biol.* **150**, 155-164.

Venkataraman, K. and Futerman, A. H. (2000). Ceramide as a second messenger: sticky solutions to sticky problems. *Trends Cell Biol* **10**, 408-412.

Vercammen, D., Beyaert, R., Denecker, G., Goossens, V., van Loo, G., Declercq, W., Grooten, J., Fiers, W. and Vandenabeele, P. (1998a). Inhibition of caspases increases the sensitivity of L929 cells to necrosis mediated by tumor necrosis factor. *J. Exp. Med.* **187**, 1477-1485.

Vercammen, D., Brouckaert, G., Denecker, G., van de Craen, M., Declercq, W., Fiers, W. and Vandenabeele, P. (1998b). Dual signaling of the Fas receptor: initiation of both apoptotic and necrotic cell death pathways. *J. Exp. Med.* **188**, 919-930.

Walsh, J. P. and Bell, R. M. (1986). sn-1,2-Diacylglycerol kinase of *Escherichia coli*. Mixed micellar analysis of the phospholipid cofactor requirement and divalent cation dependence. *J. Biol. Chem.* **261**, 6239-6247.

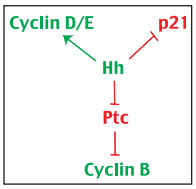

Hedgehog pedals the cell cycle

Hedgehog proteins are secreted signalling molecules that play crucial roles in pattern formation during early embryonic and post-embryonic development. Hedgehog signalling has a profound effect on cell fate but can also stimulate cell proliferation in certain developmental contexts – for example, during development of the cerebellum, Sonic hedgehog released by Purkinje neurons stimulates proliferation of cerebellar granule neuron precursors (CGNPs). In a Commentary on p. 4393, Sudipto Roy and Philip Ingham discuss the molecular mechanisms underlying control of the cell cycle by Hedgehog proteins. Studies of primary CGNP cultures, knockout work and gene expression profiling indicate that Hedgehog signalling can stimulate synthesis of D-type cyclins, which inactivate the tumour suppressor RB and thereby promote S phase entry. Genetic analysis of the 'second mitotic wave' during fly eye development has revealed that Hedgehog can similarly induce expression of cyclin E, which also targets RB. An interesting twist is the observation that the vertebrate Hedgehog receptor PTC1 directly interacts with and sequesters the G2/M-controlling cyclin, cyclin B1. Hedgehog signalling could therefore promote M-phase progression as well – by liberating PTC-bound cyclin B1.

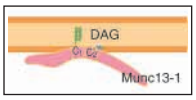

The folly of phorbol ester

Activation of protein kinase C (PKC) by diacylglycerol generated through hydrolysis of phosphatidylinositol 4,5-bisphosphate is a classic signal transduction mechanism. Indeed, cell biologists and pharmacologists have over the years used the diacylglycerol analogue phorbol ester to implicate PKC in a wide variety of processes. Recent work, however, indicates that diacylglycerol and phorbol ester have additional targets, such as chimaerins, the Ras activator RasGRP and the vesicle-priming protein Munc-13. In a Commentary on p. 4399, Nils Brose and Christian Rosenmund review the evidence for such non-PKC targets. These proteins each contain the diacylglycerol-binding C_1 domain and function in processes in which PKCs were previously implicated. Release of neurotransmitter from hippocampal neurons, for example, is regulated by phorbol ester, but since neurons expressing a Munc-13 C_1-domain mutant cannot respond to phorbol ester the target must be Munc-13. Similar work indicates that RasGRP – and not PKC – couples T cell receptors to MAP kinase activation in thymocytes. Brose and Rosenmund conclude that susceptibility to phorbol esters does not alone constitute a test for PKC involvement and discuss additional criteria that should be satisfied.

Overriding MAP kinase

Transduction of extracellular signals that stimulate cell proliferation requires the small GTPase Ras. Precisely which Ras signalling pathways are involved remains obscure, however, given the numerous potential Ras effectors (e.g. Raf, PI3 kinase and phospholipase Cε) and doubts concerning the validity of the overexpression studies often used to define them. Chris Marshall and co-workers have now dissected mitogenic signalling through Ras by examining the requirement for ERK (part of the Ras-Raf-MEK-ERK MAP kinase cascade) signalling in cells lacking the tumour suppressor RB, using inhibitors of MEK to block ERK activation. Among their results is the observation that, unlike wild-type cells, $RB^{-/-}$ mouse embryonic fibroblasts do not require significant ERK activation for exit from G0 phase and entry into S phase (see p. 4607). Since $RB^{-/-}$ cells require Ras for exit from G0, this key finding indicates that although Ras/ERK signalling is required for the G1/S transition, an ERK-independent Ras mechanism drives exit from G0. It also demonstrates – for the first time – that loss of a tumour suppressor can alter cellular requirements for MAP kinase signalling.

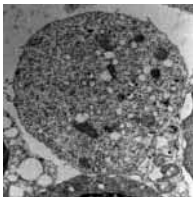

Apoptosis vs necrosis: ceramide decides it

Cells that apoptose yield vesicles without releasing their content. Death by necrosis, by contrast, involves cell swelling and lysis and can therefore generate inflammatory responses. But what determines whether a cell undergoes apoptosis or necrosis? Andrew Quest and co-workers have approached this question by examining Fas-induced death of A20 B lymphoma cells (see p. 4671). They observe that – as expected – Fas ligand triggers apoptosis, and this is accompanied by and dependent on activation of caspase-8 (the initiator caspase recruited to the Fas death receptor) and caspase-3 (a downstream effector caspase). Interestingly, apoptosis only occurs in ~60% of cells. The rest undergo necrosis, and this requires caspase-8 but not caspase-3. The authors also observe that death of A20 cells is accompanied by ceramide generation, which, like necrosis, requires caspase-8 but not caspase-3. Furthermore, they demonstrate that ceramide treatment can promote necrosis of lymphoid cells and that a lymphoid line that does not generate ceramide undergoes Fas-induced apoptosis but not necrosis. Ceramide thus seems to determine how the cells die, which could be important given that necrosis is critical for certain immune responses.

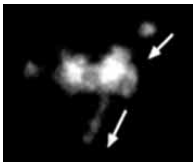

Centrosome flares

Centrosomes, the major microtubule-organizing centres in animal cells, each comprise two centrioles and a surrounding cloud of pericentriolar material (PCM). The PCM contains a filamentous 'centromatrix' plus additional proteins such as centrosomin (CNN) and is often thought to be a static structure. Thomas Kaufman and co-workers show that it can in fact be highly dynamic (see p. 4707). Imaging CNN-GFP fusion proteins in live *Drosophila* embryos, they demonstrate that particles containing CNN and another centrosomal protein, D-TACC, oscillate radially back and forth from the centrosome. These 'centrosome flares' are cell cycle regulated: flare activity decreases during metaphase, increasing again at telophase. The authors show that interfering with microtubule dynamics inhibits flaring, concluding that the process is driven by association of CNN with dynamic astral microtubules. Interestingly, during mitosis, the flares extend only as far as the actin cages surrounding the spindle; moreover, disruption of the actin cytoskeleton increases the distance flares travel, allowing them to jump to neighbouring centrosomes. The flares thus appear to be limited by the actin cage and might play a part in organizing its boundary.

Sticky Wicket – The Mole

Contributors to the Sticky Wicket column are an odd bunch. Caveman, Cavewoman Anaya, The Wicked Witch of the West and Sabretooth: they all have their idiosyncrasies and pet peeves. The newest contributor – Mole – is no exception. Mole is, however, more subversive. Revelling in anonymity, our latest correspondent reveals a passion for discovering what has been swept under the carpet of cell biology (see p. 4389).

In the next issue of JCS

Commentaries

The Ena/VASP enigma. M. Krause et al.
Apoptosis-inducing factor. C. Candé et al.

Research Articles

Interaction of tyrosylated HDL with cholesterol-laden macrophages. I. Suc et al.
Chromogranin A trafficking. L. Taupenot et al.
Effect of CMT mutations on assembly of NFs. R. Perez-Olle et al.
Myosin VI functions in actin dynamics. A. D. Rogat and K. G. Miller
NFκB activation differentially influences apoptosis. C. Fan et al.
Wnt regulation of chondrocyte differentiation. V. Church et al.
β-Catenin phosphorylation by CKII. S. Bek and R. Kemler
DNA replication competence of the xrs-5 mutant. D. Matheos et al.
Intracellular localization and dynamics of myosin-II and myosin-IC. H.-H. Kong and T. D. Pollard
Citron kinase and spermatogenesis. F. Di Cunto et al.
Claudin-2 forms paracellular cation channels. S. Amasheh et al.
Assembly of the PINCH-ILK-CH-ILKBP complex. Y. Zhang et al.
Dynein 2 in cilia. A. Mikami et al.
RA and motoneuron disease. J. Corcoran et al.
CfNek copurifies with glutamylation activity. S. Westermann and K. Weber
Acetylation of histones H4/H3 in sciarid flies. C. Goday and M. F. Ruiz
Neuritogenesis on distinct LN substrates. E. Freire et al.
Lasp-1 binds to F-actin. C. S. Chew et al.
ABA-responsive gene expression. S. Hoth et al.
SARA in Rab5-regulated endocytic trafficking. Y. Hu et al.
IP3-activated channels and tip growth. L. B. Silverman-Gavrila and R. R. Lew
DRAL/FHL-2 targeting to the sarcomere. S. Lange et al.
Cathepsin B – green fluorescent protein. M. Linke et al.
Sbh1p characterization. A. Boisramé et al.
Regulation of Lte1 localisation in budding yeast. S. Jensen et al.
Plakin cytoskeletal interactions. T. Karashima and F. M. Watt
Calcium and cell swelling in Necturus erythrocytes. D. B. Light et al.
Yck2p plasma membrane targeting. P. Babu et al.
Involvement of Chat-Cas complex in Rap1 activation. A. Sakakibara et al.
A novel family of DOCK180-related proteins. J.-F. Côté and K. Vuor